A Novel Heavy-Load Nursing Robotic Arm - Design and Safety Control Based on Tactile Skin

Yanshu Song, Jiahao Wu, Fei liu, Bing Li, Hailin Huang*, Fengfeng Xi*

Abstract— Service robots are being increasingly used to replace human beings in carrying out various sophisticated, heavy and even dangerous tasks. In order to solve the problem of labor shortage in the medical and nursing industry, this paper proposes a novel heavy-load robotic arm for nursing tasks, which can help caregivers to lift and transfer patients. Firstly, we simulate and analyze the specific nursing tasks and application scenarios, and determine its kinematics configuration and load capacity parameters of each joint. Then we design the modular and low flexibility robotic joints for it and manufacture the prototype. To avoid the occurrence of safety accidents while lifting patients, we design a new kind of tactile robotic skin based on the resistance characteristic of varistor materials, and propose a safety control algorithm based on it. Experiments show that it can meet the requirements of load capacity and position control accuracy, and the proposed safety control algorithm can effectively avoid many dangerous situations.

I. INTRODUCTION

The development of robotics technology and the shortage of labor force have resulted in a large number of assistive robots of various types. For example, Christian [1] proposed an intelligent wheelchair robot which combined a noninvasive EEG-based human-robot interface and an autonomous navigation system to help severely disabled people who cannot steer a wheelchair. LIRMM have designed a biped robot called SHERPA, which has multiple 2 DOF cable-driven differential modular joints and can deliver goods by walking [2]. Wing [3] presented a novel rescue robot system called RescueBot. It consists of a crawler-type robotic chassis and a wearable suit which allows the RescueBot replace rescue workers in performing different types of rescue tasks.

Assistive robots for nursing tasks are emerging to address the social need due to the changing demographic trends such as an ageing population. Barrett company has developed a rope-driven robot called WAM, which has six joints based on differential mechanisms and can be used to assist in the treatment of stroke [4]. Ming [5] designed a feeding assistive robot consisting of four modular flexible joints, which could meet the needs of people with upper limb disabilities or dysfunctions in gaining independence in eating. Greg presents an assistive robot to undertake dressing tasks using a compliant robotic arm on a mannequin and several strategies are explored on how to undertake this task with minimal complexity and a mix of sensors [6].

Service robots used to perform nursing tasks need to have direct contact with humans in uncertain environments, which brings great security challenges. Therefore, researches on the safety mechanisms, safety sensors and safety control methods of nursing robot have been wildly carried out to prevent accidents. Mukai et al. developed the RIBA nursing robot [7] with differential modular robotic joints which can generate greater output torque at the same joint sizes [8]. To ensure the safety of man-machine interaction, the soft materials such as polyurethane foam and tactile sensors are wrapped on the robotic arms for tactile guidance. The RONA nursing mobile robot [9] developed by Hstar Technologies is a physical assistance system that works effectively in a hospital environment under telepresence control by nurses or physicians. It has a humanoid design with bimanual dexterous manipulators employing a series-elastic-actuation (SEA) system, which can provide the manipulators compliance, safety, and the strength to lift patients weighing up to 300lbs. Waseda University proposed the human symbiotic robot TWENDY-ONE [10], which can provide physical supports to the elderly such as attendant care with high-power and kitchen supports with dexterity. The whole body of the manipulator is covered with flexible silicone materials and distribution pressure sensors ensuring that the robot can be stopped in time when dangerous situations occur.

In view of the shortage of medical staff in hospitals, this paper proposes a novel heavy-load nursing robotic arm which can be used to assist nurses in moving patients between stretchers and beds. To ensure safety, we design a new kind of tactile robotic skin based on the resistance characteristic of varistor materials, and propose a safety control method based on it. Experiments have verified that the manipulator and the tactile skin can meet requirements of load capacity for nursing tasks and accuracy of pressure measurement, respectively. The proposed safety control algorithm can also effectively avoid the occurrence of dangerous situations in the process of man-machine interaction.

This paper is organized as follows. Section II and III introduce the design and manufacture of the heavy-load robotic arm and the soft tactile skin, respectively. Section IV describes the proposed safety control method to avoid the occurrence of dangerous situations in nursing process. Three groups of experiments were conducted and the analysis of results is presented in Section V. Finally, Section VI concludes the paper.

II. MECHANICAL DESIGN

A. Requirement analysis

The robotic arm is mainly used in hospitals and nursing rooms to lift and transfer patients. Considering the complexity of the working environment and the requirement of adapting patients' postures, we determine the degree of the freedom of the manipulator arm to be 6. The joints placements are designed referring to the human arm, as shown in Fig. 1.
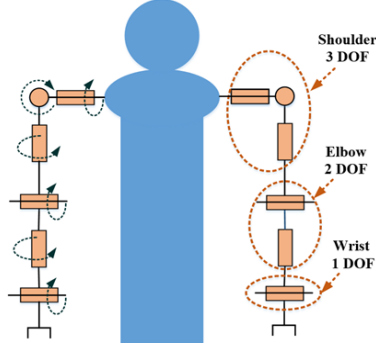

Fig. 1. Diagram of robotic arm's joints placements

This nursing robotic arm is used to carry out the task of lifting and moving patients, so the basis of ensuring its safety is that the selected motors, reducers and other components can meet the strength requirements. We build a dynamic simulation model based on Adams to obtain the maximum load torque of each joint. In order to enable the manipulator arm to complete nursing tasks in various environments, we set simulation constraint parameters according to the most extreme conditions. As shown in Fig. 2, the length of the upper arm is 500mm and its quality is 15kg; the length of the lower arm is 500mm and its quality is 10kg; and finally the block pressed on the center of the lower arm is 50kg.

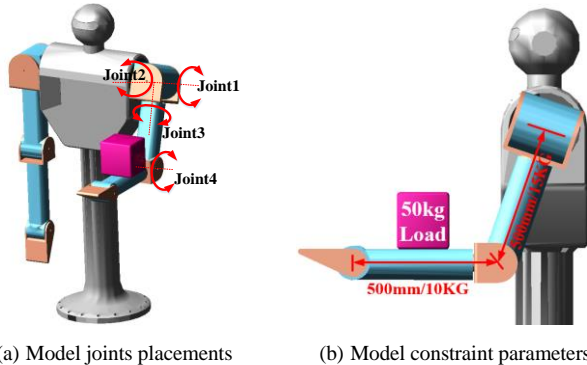(a) Model joints placements   (b) Model constraint parameters

Fig. 2. Dynamic simulation model

When the manipulator arm lifts the load with different postures and accelerations in the simulation environment, the maximum output torques and rotation angle ranges of the first four joints are shown in Table 1.

Table 1 Design parameters of the first four joints

Joint	Maximum output torque (Nm)	Rotation angle range (degree)
Joint 1	471.2	-90-90
Joint 2	252.1	0-90
Joint 3	124.6	-90-90
Joint 4	147.3	-90-90

B. Mechanical structure

The upper arm consists of four joints, as shown in Fig. 3. The first two joints adopt the traditional arrangement method of serial manipulator, selecting the suitable DC brushless motor, harmonic reducer and servo driver according to the design parameters, and installing them sequentially. Compared with other types of reducers, harmonic reducer has the advantages of large deceleration ratio and strong load-carrying capacity, but it also brings greater flexibility to the robotic joint. Therefore, we equip the joint with high-precision magnetic grating encoder both at the motor side and the output side of the harmonic reducer to improve the accuracy of its position control. In addition, we design a frictional brake at the end of each motor, so that the robot can hold the patients stably and safety in the event of a power failure.
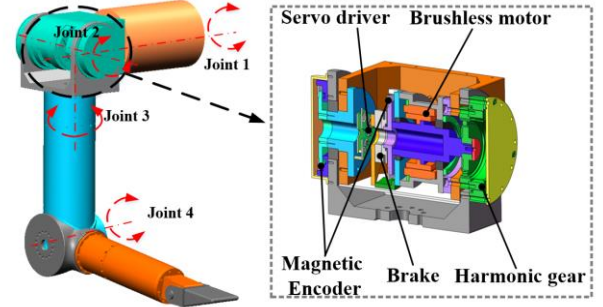

Fig. 3. The traditional robotic joint arrangement method

In order to obtain high torque density and improve space utilization, joint 3 and joint 4 are arranged symmetrically in reverse direction in the same shell. At the same time, we design a multi-stage deceleration mechanism for each joint to improve its output torque. As shown in Fig. 4, the brushless DC motors (Maxon EC 52) are staggered on the shell. The motor of joint 3 is connected to a planetary reducer to achieve the first stage deceleration and then connected to a pair of spur gears to achieve the second stage deceleration. Finally, it is connected to a hollow harmonic reducer to realize the third stage deceleration and output torque and motion. Similarly, the motor of joint 4 achieves the first stage deceleration through a planetary reducer, and changes its direction by a pair of bevel gears, and finally is connected to a harmonic reducer to achieve a larger torque output. The total deceleration ratio of the motion transmission of both joints is 520:1. In order to avoid the influence of backlash in gear transmission on the accuracy of position control, we also design high-precision encoders both at motor sides and output sides of the two joints. And the joint 4 is equipped with frictional brake to ensure safety. The cross section and prototype of the two joints are shown in Fig. 4 and Fig. 5, respectively.
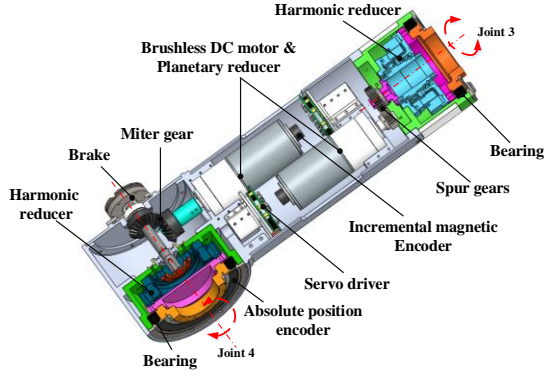
Fig. 4. The cross section of the joint 3 and the joint 4

Fig. 5. The prototype of the joint 3 and the joint 4

The cross section of the lower arm is shown in Fig. 6, which consists of the joint 5 and the joint 6. In joint 5, the brushless motor is directly connected with a harmonic reducer to achieve single-stage deceleration and output motion. For joint 6, the motor achieves the first stage deceleration through a planetary reducer, and then it is connected to a right-angle reducer to realize the second stage deceleration and the change of the rotation direction. Each joint of the manipulator arm adopts hollow design form to ensure that the cable can be completely wrapped in the interior of the robot. The servo actuator of each joint is installed inside the joint and transmit signals through CAN bus.
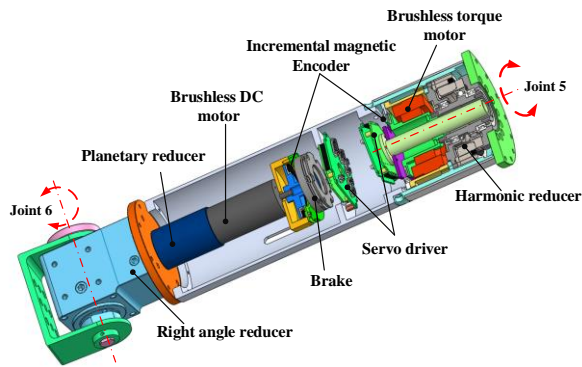

Fig. 6. The cross section of the lower arm

III.   TACTELE SKIN DESIGN

A. Sensing principle

In order to detect the magnitude of the pressure acting on

the manipulator and the position of the pressure acting point to make the manipulator carry out the task of lifting and transferring patients safely, we design a novel kind of flexible robotic skin which has tactile function. Its core component is the membrane-structured matrix of piezoresistive flexible film sensors produced by transferring nano-sensitive materials and silver paste to flexible film substrates through a precise printing process. Each sensor matrix consists of 8×8 detection units, and the conductivity of the detection unit has a linear relationship with the pressure. Each unit has a size of $12 \text{ mm} \times 12 \text{mm}$, a measuring range of 0-5 kg, and a response time of 10 ms.

To protect the resistive pressure elements from damage, we embed them in pieces of 7mm thick honeycomb skin substrates which are processed by 3D printing using skin-friendly photosensitive resin Nitrile Butadiene Rubber (NBR) and used as buffers between the patient and the rigid robotic arm. The buffer layer consists of two rows of staggered hexagonal holes to achieve better cushion and minimize total weight while maintaining the structural strength [11]. In addition, the stiffness of the honeycomb substrate can be modified by adjusting the thickness and size of the hexagonal cell to obtain better performance of shock attenuation [12]. NBR is selected because of its chemical stability, suitable elasticity, and ease of manufacture, making the tactile skin be able to attach to any curved surface.

This new tactile skin is wrapped around the upper arm and the lower arm of the manipulator, which not only enables the manipulator to perceive the pressure from various positions, but also provides a more comfortable experience [13] when contacting with patients. Its structure and the placement positions are shown in Fig. 7.
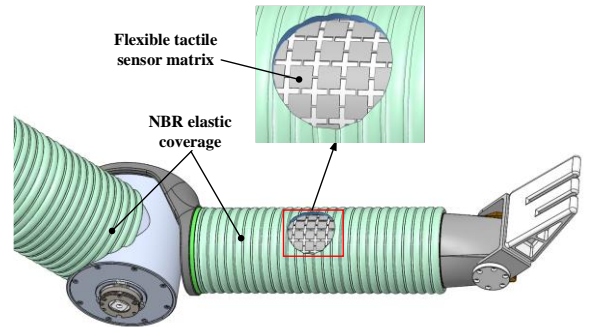

Fig. 7. The structure of the new tactile skin and its placement positions

According to the actual size of the manipulator, each arm needs to be wrapped with 10 pieces of tactile skin and each piece of tactile skin contains 64 detection units, which require a large number of wires to transmit current signals. In order to reduce the number of long wires and avoid the problem of signal interference caused by a large amount of interlaced wires, we equip every two pieces of tactile skin with one current signal acquisition board. Based on the resistance characteristics of pressure sensor unit, it can collect current signals of 64×2 units at the same time and convert them into digital signals through A/D converter circuit. Finally, it transmits these signals to the main control board through CAN

bus. The highest acquisition frequency is 200hz and the connection between the acquisition board and the two pieces of tactile skin is shown in Fig. 8.
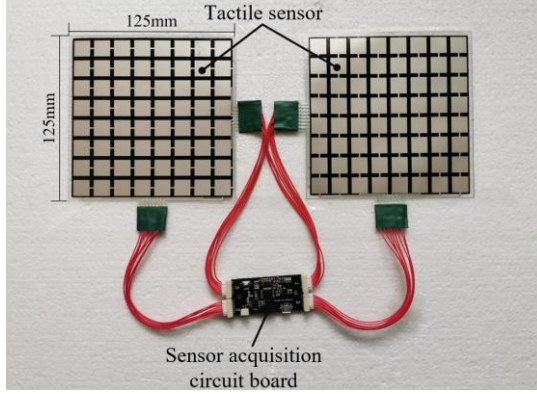

Fig. 8. The connection of the acquisition board

B. *Sensing calibration*

In theory, the resistance of the pressure sensor unit has a definite non-linear relationship with the pressure, so we design an experimental platform to calibrate it. As shown in Fig. 9(a), the applied pressure values are measured by high-precision digital pressure sensor, and the corresponding resistance values of pressure sensor units are measured by a multi-meter. Because the resistance variation characteristics of different units have little difference, we randomly select 10 cells and average the measured resistance and pressure values for convenience. The actual relationship between the resistance of the pressure sensor unit and the pressure is shown in Fig. 9(b). It can be seen that the resistance decreases with the increase of the pressure, while the relationship between conductivity and pressure is very linear. We get the numerical relationship between them by fitting the data, as shown in equation (1).
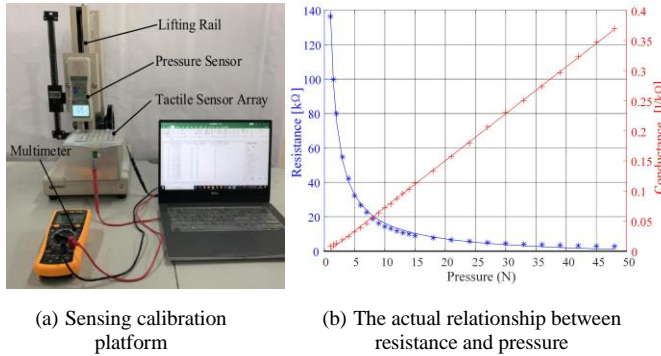

(a) Sensing calibration platform   (b) The actual relationship between resistance and pressure

Fig. 9. Sensing calibration process

$$F = 27.9 \times R^{-0.97} + 0.3479 \qquad (1)$$

Where F is the pressure applied on the pressure sensor unit and R denotes the corresponding resistance. So when the manipulator is in contact with the patients, the pressure on each pressure sensor unit can be calculated by equation (1).

IV. SAFETY CONTROL SYSTEM

A. *Control system design*

As shown in Fig. 10, the main controller of the manipulator arm is designed based on the Robot Operating System (ROS) [14]，which makes it more convenient to handle tasks such as hardware abstraction, message-passing between processes, low-level device control and package management. In motor control, each joint is equipped with an independent servo driver, which controls the movement of the brushless DC motor through the 402 protocol of CAN-open and communicates with the main controller through USB to CAN. Similarly, the current signals in 10 pieces of tactile skin are collected and processed into pressure signals through five acquisition boards, and then transmitted to the main control board through CAN bus. The main control board receives the pressure information on each tactile skin, and then makes decisions based on our proposed security algorithm, and finally sends motor motion control instructions to each servo driver.
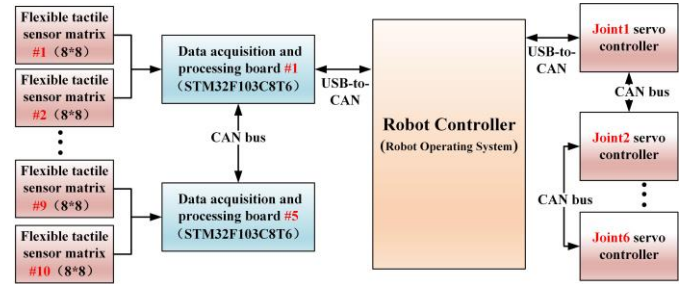

Fig. 10. The control system of the manipulator arm

B. *Safety control method*

Due to the limitation of the physical structure of the manipulator, the payload of each arm is 50kg and the contact force need to act on the center of the lower arm as shown in Fig. 12 (a). However, the following dangerous situations may occur during the process of lifting and transferring the patient (Fig. 11):

(a) During the process of lifting a patient, the patient's center of gravity is too far ahead of the manipulator arm.

(b) During the process of transferring a patient, the patient's center of gravity is too biased towards one of the double arms.

(c) The patient's weight exceeds the payload of the manipulator arm.

These situations can overload the manipulator arm and even cause the patient to fall off from the arm, which are major safety accidents.

(a) Too far ahead of the arm situation   (b) Too biased towards one side situation   (c) Weight exceeds the payload situation
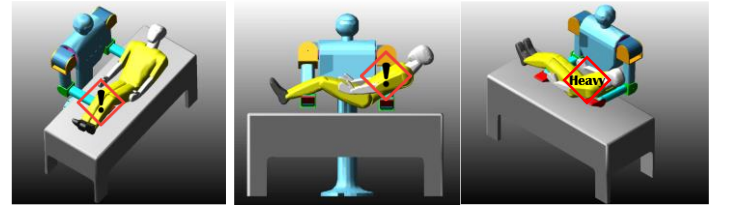
Fig. 11. Dangerous situations while lifting and transferring the patient

As shown in Fig. 12 (b), the manipulator arm has three types of postures when contacting with patients, i.e. the initial pose, the contact pose, the lift pose. In order to prevent the

occurrence of the above dangerous situations, we propose a safety control method which can imitate the human mind and make motion decisions.

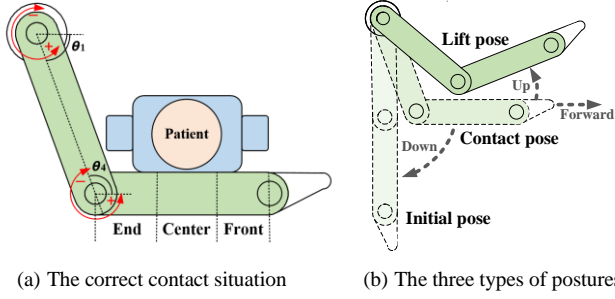(a) The correct contact situation   (b) The three types of postures

Fig. 12. Postures of the robotic arm in task execution

Firstly, when the manipulator is in contact with the patient, the tactile skin wrapped in different positions of the arm can sense different sizes of pressure. So the patient's gravity and real-time gravity center position can be calculated by the equation (2) and equation (3).

$$G_L = \sum G_{ij} \tag{2}$$

$$P_L = \frac{\sum G_{ij} \cdot P_{ij}}{G_L} \quad i, j \in [1, 2, 3 \cdots, 8] \tag{3}$$

Where G_{ij} is the force detected by the pressure sensor unit in the i-th row and the j-th column of the tactile robotic skin, G_L is gravity of the patient, P_{ij} is the position vector of the corresponding unit, and P_L denotes the position of the center of gravity of the patient.

After the gravity and the position of the center of gravity are detected, the main control board will indicate the movement of each joint according to the following rules:

(1) In the process of lifting a patient: if it is detected that the load of each arm is greater than 50 kg, the arm will slowly put the patient down and sound an alarm.

(2) In the process of transferring a patient: if it is detected that the patient's center of gravity is in the first third of the lower arm, the arm will be slowly put down and stretch forward until the patient's center of gravity is adjusted in the middle of the arm.

The flow chart of this safety control method is shown in Fig. 13. Using the control strategies can ensure that the patient does not slip or fall from the robotic arm during the lifting and transferring processes, thereby ensuring the safety when the manipulator arm carrying out the nursing task.
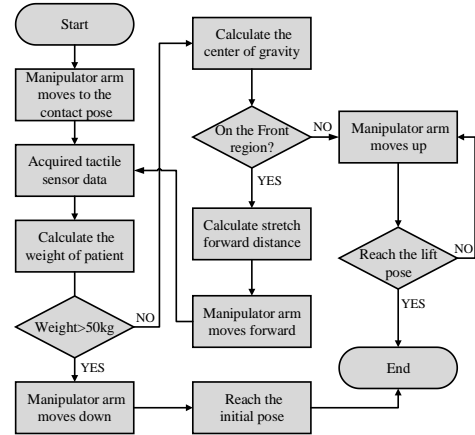

Fig. 13. The flow chart of the safety control method

V. EXPERIMENTS AND RESULTS

A. Load capability

This manipulator arm needs to be able to carry the weight of a patient when performing nursing tasks, that is to say, the single arm can carry a load of 50 kg. As shown in Fig. 14, we fix the manipulator on a stationary vibration isolation platform, and then hang a 50 kg weight on its lower arm with nylon rope. It can be seen that the manipulator can lift the weight smoothly, so it can meet the design requirements.
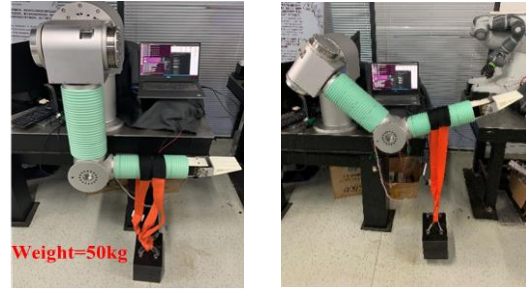

(a) The initial state   (b) Lifting the load weight

Fig. 14. The load capability test platform

B. Tactile skin performance

To test the perception performance of the proposed tactile skin, we connect two pieces of the robotic skin on the same plane and place a weight of 10 kg on them as shown in Fig. 15 (a). The Fig. 15 (b) shows the pressures measured by each pressure sensing unit and the highest prism represents the calculated center of gravity of the load. It can be seen that the pressure distribution measured is consistent with the actual situation, and the difference in measurements between the sensing units at symmetrical position is less than 5%.
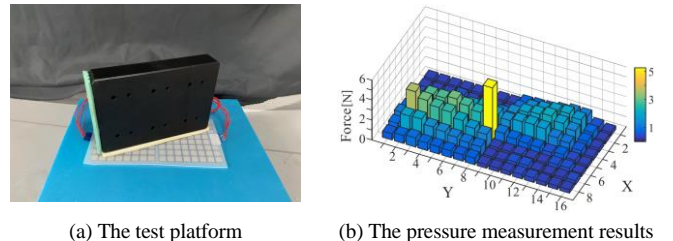

(a) The test platform   (b) The pressure measurement results

Fig. 15. Tactile skin performance test

C. Safety control

In order to verify the proposed safety algorithm based on tactile skin, we press the different areas of the manipulator to simulate the patient's contact with it. The specific experimental process is as follow:

(1) Firstly, the manipulator moves from the initial position shown in Fig. 16 (a) to the posture shown in Fig. 16 (b) to prepare to lift the patient.

(2) Then pressing the front side of the lower arm, the pressure distribution perceived by the tactile skin is shown in Fig. 17 (a). The main control board processes this information and gets that the center of gravity of the load is in the first third of the arm, so the arm automatically adjusts its posture forward as shown in Fig. 16 (c).

(3) Finally, pressing the middle of the lower arm with force less than 50 kg after the manipulator adjusts its posture. The pressure distribution perceived by tactile skin is shown in Fig. 17 (b). The main control board processes this information and concludes that the load size and the position of action point are both safe, so it performs the action of lifting the patient up as shown in Fig. 16 (d).

Fig. 18 shows the angular position changes of the two main joints during the whole experimental process. The result shows that the main control board can calculate the total load and its position of the center of gravity accurately through the pressure distribution information measured by the tactile skin. And it can guide the manipulator to make appropriate movement according to the proposed safety control method, thus realizing the safe implementation of nursing tasks.

(a) Initial pose

（b）Pressing the front region

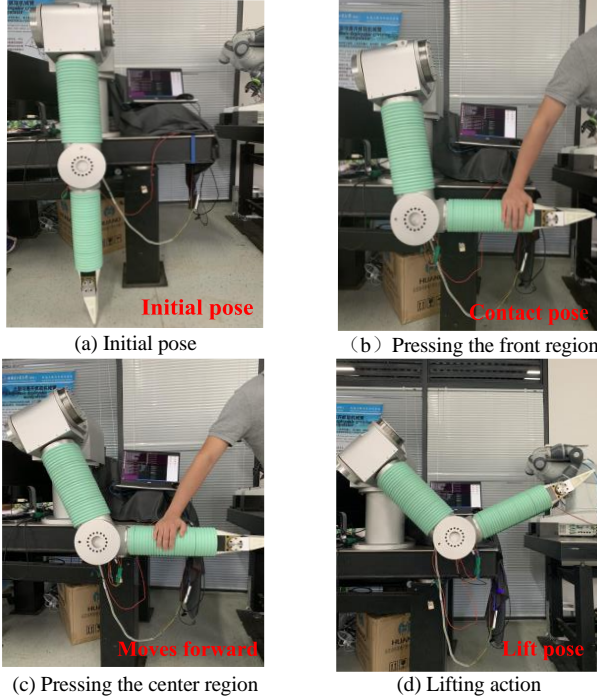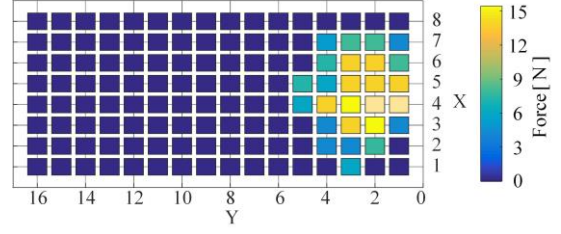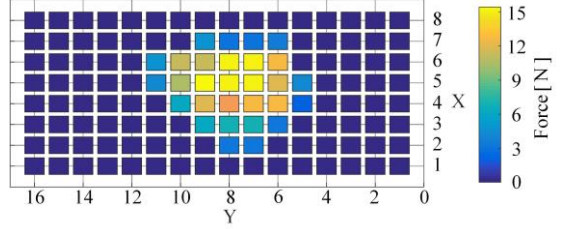(c) Pressing the center region

(d) Lifting action

Fig. 16. The experimental process of safety control

(a) The pressure distribution when pressing the front region

(b) The pressure distribution when pressing the center region

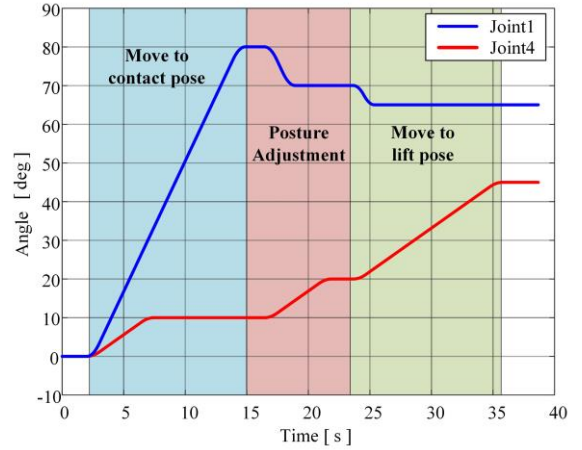Fig. 17. The pressure distribution perceived by the tactile skin

Fig. 18. The angular changes of joint 1 and joint 4

VI. CONCLUSION

In this paper, we design a novel heavy-load manipulator arm for nursing tasks. In order to ensure the safety of the manipulator contacting with patients, we design a novel kind of robotic skin with tactile perception function and propose a safety control system. Experiments show that our manipulator arm can meet the requirement of carrying capacity, and the designed tactile robotic skin can measure the pressure distribution accurately. Finally, our safety control system can effectively avoid the occurrence of some dangerous situations. The tactile skin and the safety control strategy proposed in this paper will help to improve the comfort and safety in the process of human-machine interaction. However, there are still some problems, such as the inconsistencies in resistance characteristics, the low resolution of pressure sensing, and the invalidation of the tactile skin edges. Further work will focus on solving these problems and making it more general, more accurate and easier to use.

REFERENCES

[1] C. Mandel, T. Lüth, T. Laue, T. Röfer, A. Gräser and B.Krieg-Brückner, "Navigating a smart wheelchair with a brain-computer interface interpreting steady-state visual evoked potentials," 2009 IEEE/RSJ International Conference on Intelligent Robots and Systems, St. Louis, MO, 2009, pp. 1118-1125.

[2] Ionut Mihai Constantin Olaru Franc ̦ois Pierrot, Sebastien Krut. Novel mechanical design of biped robot sherpa using 2 dof cable differential modular joints. In Intelligent Robots and Systems, 2009 IEEE/RSJ International Conference on, pages 4463–4468. IEEE, 2009.

[3] W. K. Chung, Y. Yang, N. Cui, H. Qian and Y. Xu, "Design of a rescue robot with a wearable suit augmenting high payloads rescue missions," 2017 2nd International Conference on Advanced Robotics and Mechatronics (ICARM), Hefei, 2017, pp. 704-711.

[4] Ian Sharp, James Patton, Molly Listenberger, and Emily Case. Haptic/graphic rehabilitation: Integrating a robot into a virtual environment library and applying it to stroke therapy. Journal of Visualized Experiments: JoVE, (54), 2011.

[5] M. Guo, P. Shi and H. Yu, "Development a feeding assistive robot for eating assist," 2017 2nd Asia-Pacific Con-ference on Intelligent Robot Systems (ACIRS), Wuhan, 2017, pp. 299-304.

[6] G. Chance, A. Camilleri, B. Winstone, P. Caleb-Solly and S. Dogramadzi, "An assistive robot to support dressing - strategies for planning and error handling," 2016 6th IEEE International Conference on Biomedical Robotics and Biomechatronics (BioRob), Singapore, 2016, pp. 774-780.

[7] T. Mukai et al., "Development of a nursing-care assistant robot RIBA that can lift a human in its arms," 2010 IEEE/RSJ International Conference on Intelligent Robots and Systems, Taipei, 2010, pp. 5996-6001.

[8] K. Wang, H. Qian, Y. Yang and Y. Xu, "A novel Differential Modular Robot Joint — Design and implementation," 2013 IEEE International Conference on Robotics and Biomimetics (ROBIO), Shenzhen, 2013, pp. 2049-2054.

[9] J. Hu et al., "An advanced medical robotic system augmenting healthcare capabilities - robotic nursing assistant," 2011 IEEE International Conference on Robotics and Automation, Shanghai, 2011, pp. 6264-6269.

[10] H. Iwata and S. Sugano, "Design of human symbiotic robot TWENDY-ONE," 2009 IEEE International Conference on Robotics and Automation, Kobe, 2009, pp. 580-586.E. H. Miller, "A note on reflector arrays (Periodical style—Accepted for publication)," IEEE Trans. Antennas Propagat., to be published.

[11] S. Belouettar, A. Abbadi, Z. Azari, R. Belouettar, and P. Freres, "Experimental investigation of static and fatigue behaviour of composites honeycomb materials using four point bending tests," Composite Structures, vol. 87, no. 3, pp. 265–273, 2009.

[12] Y. Ning, R. Niu, S. Wang, and B. Li, "A new kind of non-pneumatic tire for attenuating vibration," in 2016 IEEE International Conference on Robotics and Biomimetics (ROBIO). IEEE, 2016, pp. 1601–1606.

[13] Y. Ohmura, Y. Kuniyoshi, and A. Nagakubo, "Conformable and scalable tactile sensor skin for curved surfaces," in Proceedings 2006 IEEE International Conference on Robotics and Automation, 2006. ICRA 2006. IEEE, 2006, pp. 1348–1353.

[14] Quigley M, Gerkey B P, Conley K, et al, "ROS: An open-source Robot Operating System[J]," 2009.